Environmental Science & Technology

Article

pubs.acs.org/est

Microbial Extracellular Polymeric Substances Reduce Ag^+ to Silver Nanoparticles and Antagonize Bactericidal Activity

Fuxing Kang,[†] Pedro J. Alvarez,[‡] and Dongqiang Zhu*[,†]

[†]State Key Laboratory of Pollution Control and Resource Reuse/School of the Environment, Nanjing University, Nanjing, Jiangsu 210046, People's Republic of China

[‡]Department of Civil and Environmental Engineering, Rice University, Houston, Texas 77251, United States

Supporting Information

ABSTRACT: Whereas the antimicrobial mechanisms of silver have been extensively studied and exploited for numerous applications, little is known about the associated bacterial adaptation and defense mechanisms that could hinder disinfection efficacy or mitigate unintended impacts to microbial ecosystem services associated with silver release to the environment. Here, we demonstrate that extracellular polymeric substances (EPS) produced by bacteria constitute a permeability barrier with reducing constituents that mitigate the antibacterial activity of silver ions (Ag^+). Specifically, manipulation of EPS in *Escherichia coli* suspensions (e.g., removal of EPS attached to cells by sonication/centrifugation or addition of EPS at 200 mg L^{-1}) demonstrated its critical role in hindering intracellular silver penetration and enhancing cell growth in the presence of Ag^+ (up to 0.19 mg L^{-1}). High-resolution transmission electron microscopy (HRTEM) combined with X-ray photoelectron spectroscopy (XPS) and energy-dispersive spectrometry (EDS) analyses showed that Ag^+ was reduced to silver nanoparticles (AgNPs; 10−30 nm in diameter) that were immobilized within the EPS matrix. Fourier transform infrared (FTIR) and ^{13}C nuclear magnetic resonance (NMR) spectra suggest that Ag^+ reduction to AgNPs by the hemiacetal groups of sugars in EPS contributed to immobilization. Accordingly, the amount and composition of EPS produced have important implications on the bactericidal efficacy and potential environmental impacts of Ag^+.

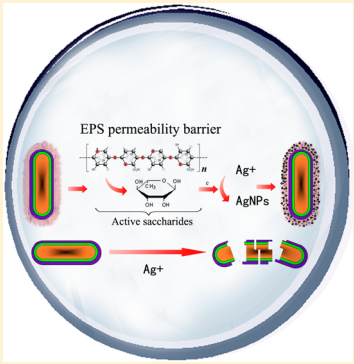

INTRODUCTION

Various silver compounds and silver nanoparticles (AgNPs) are being increasingly used in a wide range of applications, including medical, bactericidal, and electrical products.[1] This raises the likelihood of incidental and accidental release of silver to the environment and underscores the importance to understand bacterial adaptation and defense mechanisms that could mitigate unintended impacts to microbial ecosystem services or hinder antimicrobial applications.

Recent research has demonstrated that released silver ions (Ag^+) are the critical effectors of the antimicrobial activity of AgNPs.[2] Ag^+ is one of the most toxic metal cations to bacteria,[3] in part because of its strong affinity to proteins and nucleic acids, particularly to thiol groups in proteins (e.g., cysteine−SH). However, Ag^+ has a higher propensity than AgNPs to be scavenged by inorganic ligands and organic matter in aqueous systems, making AgNPs often an effective vehicle to deliver Ag^+ to bacteria.[4]

Whereas microbial physiologic adaptation and defense mechanisms to cope with Ag^+ are poorly understood, previous work with other toxic heavy metals suggests that extracellular polymeric substances (EPS) secreted by bacteria could play a significant protective role.[5] Bacteria can secrete and embed themselves in EPS that are comprised mostly of polysaccharides and proteins.[6,7] EPS play key roles in cell surface attachment and microhabitat formation to protect cells against environmental stresses, such as desiccation, predation, antibiotic agents, high salinity, and extreme temperature and pH conditions.[7−9] Because of the large content of chelating groups (e.g., amino, carboxyl, and phenol), EPS can effectively bind heavy metal cations (such as Cu^{2+}, Pb^{2+}, and Zn^{2+}) and act as a permeability barrier to hinder intracellular penetration of the metal, thus attenuating toxicity.[5] EPS can also reduce high-oxidation-state metals, such as U^{VI} and Cr^{VI}, which are subsequently immobilized on the cell surface,[10,11] although the underlying reduction mechanisms are not fully understood.

This study provides the first direct evidence that EPS secreted by *Escherichia coli* can reduce Ag^+ and entrap it as AgNPs, thus serving as a permeability barrier to hinder intracellular penetration by silver. The EPS content of *E. coli* suspensions exposed to Ag^+ was manipulated to demonstrate the critical role of EPS in mitigating silver uptake and toxic effects. Combined spectroscopic analyses using high-resolution transmission electron microscope (HRTEM), selected area electron diffraction (SAED), X-ray photoelectron spectroscopy (XPS), and energy-dispersive spectroscopy (EDS) corroborated the formation of AgNPs from Ag^+ both in the presence of

Received: August 26, 2013
Revised: November 12, 2013
Accepted: December 12, 2013
Published: December 12, 2013

E. coli and *in vitro* with aqueous EPS. Fourier-transform infrared (FTIR) and solution-phase ^{13}C nuclear magnetic resonance (NMR) analyses were performed to identify the structural components in EPS responsible for Ag^+ reduction and immobilization.

MATERIALS AND METHODS

Materials. Triton X-114 (polyethylene glycol *tert*-octylphenyl ether, TX-114) was purchased from Acros Organics (Geel, Belgium). Nitric acid (65%), hydrogen peroxide (20%), and silver nitrate (99%) were purchased from Merck (Darmstadt, Germany). Sodium thiosulfate of guaranteed reagent grade was purchased from Sigma-Aldrich (St. Louis, MO). Ultrapure water (electric conductivity of 18.2 MΩ cm) produced by a Milli-Q gradient system (Millipore, Bedford, MA) was used to perform all experiments. Tris-(hydroxymethyl)aminomethane (Tris) was purchased from Amresco Co., Ltd. (Amresco, Solon, OH). Other chemicals used to prepare the chloride-free bacterial cultural medium were purchased from Nanjing Chemical Reagent Co., Ltd. (Nanshi, China).

Chloride-free medium was used in this work to culture Gram-negative *E. coli* K12. The medium contained[3] 40 μM Tris, 28 μM $K_2HPO_4{\cdot}H_2O$, 2.2 μM $KH_2PO_4{\cdot}3H_2O$, 18.7 μM NH_4NO_3, 9.9 μM succinic acid, 0.001 μM $CaSO_4$, 2.0 μM K_2SO_4, 1.0 μM $MgSO_4{\cdot}7H_2O$, and 10 mL/L chloride-free trace element solution. The chloride-free trace element solution (pH 7−8) contained 5.0 g L^{-1} $Na_2EDTA{\cdot}H_2O$, 0.37 g L^{-1} $Fe_2(SO_4)_3$, 0.05 g L^{-1} ZnO, 0.015 g L^{-1} $CuSO_4{\cdot}5H_2O$, 0.01 g L^{-1} $Co(NO_3)_2{\cdot}6H_2O$, 0.01 g L^{-1} $(NH_4)_6Mo_7O_{24}{\cdot}4H_2O$, and 0.01 g L^{-1} H_3BO_3. The pH of the medium was adjusted to 7.4 with sulfuric acid.

EPS Extraction. *E. coli* K12 was initially cultured in 20 mL of chloride-free medium at 37 °C for 12 h and then transferred to 1 L of fresh medium and grown for another 48 h to reach the stable growth phase (see cell growth curve in Figure S1 of the Supporting Information). The bacteria were separated from the medium by centrifugation (6000*g* at 4 °C), followed by repeated washing with Milli-Q water until the ultraviolet (UV) absorbance (280 nm) of the supernatant was constant (less than 0.01). The bacteria were then suspended to 50% of the original volume (about 1.3 × 10^8 cell mL^{-1}). EPS were extracted from the bacterial suspension, as described in the literature,[12] with a slight modification. The suspension was first processed by ultrasound with an intensity of 2.7 W cm^2 at a frequency of 40 kHz at 4 °C for 10 min to separate EPS from the pure cells and then centrifuged at 10600*g* at 4 °C for 20 min to separate the cells. The supernatant was collected and filtered through a 0.45 μm membrane (Anpel) to remove unsettled cells. The filtrate (aqueous EPS) was stored at 4 °C for later chemical analyses. The extracted aqueous EPS were freeze-dried at −65 °C and stored at −30 °C for later batch reaction experiments within 1 week.

The total organic carbon (TOC) content (20.83 mg L^{-1}) of EPS solution was measured on a TOC-5000A (Shimadzu, Kyoto, Japan). The dry weight of EPS (after drying at 105 °C for 24 h) was 58.36 mg L^{-1}. The content of protein (97.33 mg g^{-1}) in EPS was measured by the Lowry method[13] using bovine serum albumin as the standard. The content of humic acid (3.60 mg g^{-1}) was measured by the modified Lowry method[14] using a commercial humic acid (Fluka) as the standard. The content of carbohydrate (309.41 mg g^{-1}) was determined by the phenol−sulfuric acid method[15] using glucose as the standard. The content of DNA (0.52 mg g^{-1}) was measured by the diphenylamine colorimetric method[16] using calf thymus DNA as the standard. These contents were in agreement with previous reports.[17] The low DNA content in EPS indicated negligible cell lysis during the EPS extraction.

Effect of EPS on *E. coli* Growth. The effect of EPS content on *E. coli* growth was investigated in the presence of various Ag^+ concentrations. To initiate the bacterial growth experiments, 200 mL of chloride-free medium was added to a 250 mL glass conical flask equipped with a permeable silica gel stopper, followed by aqueous stock solutions of Ag^+ (200 mg L^{-1}) to obtain the desired Ag^+ concentrations (0−0.25 mg L^{-1}). The volume ratio of Ag^+ stock solution, if added, was kept below 0.1%. The bacterial growth was monitored under three different EPS conditions, namely, low EPS, medium EPS, and high EPS. The low EPS culture refers to inoculation of *E. coli* cells with removal of their own EPS using the above-mentioned sonication/centrifugation method. The high EPS culture refers to inoculation of *E. coli* cells incubated in extra aqueous EPS (200 mg L^{-1}, dry weight basis). The medium EPS (control) refers to inoculation of *E. coli* cells without manipulation of EPS. For the three different EPS conditions, the cell density (*E. coli* survival) was initially inoculated equally at 1.3 × 10^7 cell mL^{-1}. The samples were incubated and shaken in an orbital shaker in the dark at 37 ± 0.5 °C. The *E. coli* cells were grown for 16 h to reach the exponential growth phase (see Figure S1 of the Supporting Information) and then harvested by centrifugation (6000*g* at 4 °C for 10 min).[18] After removal of the supernatant, the cell pellets were resuspended with Milli-Q water. The concentration (*E. coli* survival) was measured by correlating optical density (measured spectrophotometrically) to viable plate counts.[19] First, a series of bacterial suspensions were prepared separately under the same conditions as the test samples but without silver. The optical density (OD) of these suspensions was recorded by the light absorbance at 600 nm wavelength (OD_{600}) using an ultraviolet−visible (UV−vis) spectrophotometer. After dilution by 10^6-fold, 50 μL of each bacterial suspension was placed on an agar plate with chloride-free medium. The cell colonies were counted after incubation at 37 °C for 24 h. A calibration curve between the absorbance (OD_{600}) and the cell density was generated.

$$\text{cell density (cell mL}^{-1}) = (1.976\text{OD}_{600} - 0.009) \times 10^8;\quad R^2 = 0.997$$

The cell concentration (*E. coli* survival) of the sample was then determined on the basis of the obtained calibration curve according to its OD_{600} value.

Extraction and Analysis of Ag^+ and AgNPs. After bacterial growth for 16 h, the batch samples were analyzed to detect concentrations of Ag^+ and AgNPs in culture medium, EPS attached to cells, and inside cells. The bacterial suspension was filtered through a 0.45 μm membrane under vacuum, followed by repeated washing with Milli-Q water. Note that AgNPs had particle sizes of 10−30 nm in diameter (see more details below) and could readily pass through the membrane. The concentrations of AgNPs in the filtrate were analyzed using the cloud point extraction (CPE) method.[20,21] First, 1 mL of TX-114 (10%, w/v) and 0.5 mL of $Na_2S_2O_3$ (1 mol/L) were added to 100 mL of filtrate. After the pH was adjusted to 3.0 with 0.5 M HNO_3, the samples were placed in a water bath at 40 °C for 30 min. AgNPs in the sample were concentrated into the TX-114-rich phase, whereas Ag^+ was complexed with

$S_2O_3^{2-}$ and remained in the aqueous phase.[21] The two phases were separated by centrifugation at 6000*g* for 10 min. The pellets of TX-114-AgNPs were resuspended in 50 mL of Milli-Q water. The suspension containing AgNPs and the solution containing Ag^+ were both microwave-digested at 120 °C for 10 min in the presence of 0.5 mL of 65% (w/w) HNO_3 and 2 mL of 30% (w/w) H_2O_2. The samples were concentrated to approximately 10 mL and were adjusted to pH 4.0 with 0.5 M NaOH. The silver concentrations in the samples were analyzed using the electrode method with a detection limit of 10 μg L^{-1}.[20,22]

To determine Ag^+ and AgNPs in the EPS matrix, the filtered bacterial pellet was first resuspended in Milli-Q water and EPS were extracted from the bacterial suspension using the sonication/centrifugation method, as mentioned above. The supernatant containing aqueous EPS was filtered through a 0.45 μm membrane to remove unsettled cells. The filtered cells on the membrane were resuspended in Milli-Q water and filtered. Such a process was repeated at least 5 times to make sure that EPS and associated silver contents sorbed to cells were completely washed out (verified by non-detectable silver content in the final filtrate after microwave digestion). The filtrates were collected and analyzed for the concentrations of Ag^+ and AgNPs using the electrode method in combination with CPE, as described above.

After the removal of EPS and associated silver contents, the remaining cell pellets were disrupted by repeated freeze (with liquid nitrogen) and thaw for 3 cycles,[23] followed by sonication with an intensity of 6 W cm^2 at a frequency of 40 kHz at 4 °C for 10 min. The cell lysate was collected and analyzed for the concentrations of Ag^+ and AgNPs using the electrode method in combination with CPE. Triplicate samples were run for the analysis of Ag^+ and AgNPs at each added Ag^+ concentration. The data were reported as the mean ± standard deviation.

Spectroscopic Analyses of AgNPs. A separate set of experiments were performed to produce AgNPs from Ag^+ in the presence of *E. coli* cells or EPS for the purpose of structural characterization. After mixing for 16 h at 37 °C in the dark, the samples originally containing Ag^+ (0.165 mg L^{-1}) and *E. coli* cells (1.0×10^7 cell mL^{-1}) or EPS (200 mg L^{-1}) were centrifuged at 10600*g* at 4 °C for 10 min. The cell/EPS pellets were resuspended and washed with Milli-Q water. Such a centrifugation/resuspension process was repeated 3 times to adequately remove the culture medium. One portion of the pellet was placed onto a carbon-coated copper grid for transmission electron microscopy (TEM) imaging using a bright field detector on a JEM-200CX (JEOL, Japan). The image of SAED was also recorded.

The nanoparticles produced from Ag^+ in the presence of *E. coli* cells or aqueous EPS were extracted using TX-114, as mentioned above, followed by repeated washing with Milli-Q water and freeze-drying under vacuum. XPS analysis was performed on the nanoparticles at 30.0 eV pass energy in the broad survey scan and at 70.0 eV pass energy in the high-resolution scan using a PHI 5000 VersaProbe spectrometer (UlVAC-PHI, Japan).

EDS analysis was performed on nanoparticles formed from Ag^+ in the presence of *E. coli* cells using a EX-250 spectrometer (Horiba, Japan). The spectrum was recorded at 20 kV accelerating voltage and 133 eV resolution on a scanning area of 1 × 1 μm.

The UV−vis spectra of mixtures containing 0.6 g L^{-1} Ag^+ and aqueous EPS at 0, 40, 100, or 200 mg L^{-1} after mixing for 6 h at 37 °C in the dark were recorded on a UV−vis spectrometer (UV2550, Shimadzu).

FTIR and ^{13}C NMR Characterization of EPS. To identify the structural components in EPS responsible for Ag^+ reduction, FTIR and solution-phase ^{13}C NMR analyses were performed to characterize the chemical structures of EPS before and after reaction with Ag^+ for 16 h. The FTIR spectra of freeze-dried EPS mixed with KBr (mass ratio of 1:100) were acquired on a Nicolet NEXUS870 (Nicolet). Prior to the ^{13}C NMR analysis, 6 mg of EPS granule obtained by vacuum freeze-drying were dissolved in 0.5 mL of H_2O/D_2O (volume ratio of 4:1). The spectra were collected on a 600 MHz Bruker Avance (Bruker, Ettlingen, Germany) at 4 °C.

RESULTS AND DISCUSSION

EPS Enhance *E. coli* Growth in the Presence of Ag^+. Figure 1 shows the effect of EPS on the growth yield of *E. coli*

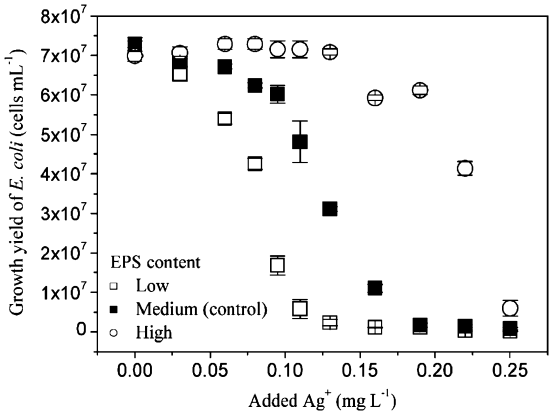

Figure 1. Effect of EPS on *E. coli* growth in the presence of various Ag^+ concentrations after 16 h of incubation. The succinate-amended chloride-free growth medium is described in the Materials and Methods. The dose−response relationships were determined under three EPS conditions: low (i.e., EPS removed by sonication/centrifugation), medium (control, no manipulation of the EPS content), and high (aqueous EPS added at 200 mg L^{-1}). For all three EPS conditions, the cell density was initially inoculated at 1.3×10^7 cell mL^{-1}. Error bars represent standard deviations calculated from triplicate samples.

(cells mL^{-1}) at various initial concentrations of Ag^+. Three treatments reflecting different EPS conditions were considered: low (EPS removed from the cells by sonication and centrifugation), medium (no manipulation of EPS content or no treatment "control"), and high (EPS added at 200 mg L^{-1}). In all treatments, the extent to which the *E. coli* concentration grew on succinate-amended chloride-free medium decreased with an increasing Ag^+ concentration, reflecting the bactericidal effect of Ag^+. Nevertheless, this inhibitory effect was significantly mitigated by EPS. For example, at an Ag^+ concentration of 0.13 mg L^{-1}, the *E. coli* population reached $(3.0 \pm 0.1) \times 10^7$ cell mL^{-1} in the control (no EPS manipulation) compared to $(5.0 \pm 0.9) \times 10^6$ cell mL^{-1} for the low-EPS treatment (83% lower) and $(7.2 \pm 0.1) \times 10^7$ cell mL^{-1} for the high-EPS set (140% higher). The enhanced effect of EPS on cell growth was not due to its potential role as a growth substrate because final cell concentrations were nearly identical for the three treatments in the absence of Ag^+ (Figure 1). Furthermore, the lethal Ag^+ concentration that killed nearly all *E. coli* cells increased with EPS content (corroborating its

protective role), from 0.16 mg L^{-1} (low EPS) to 0.25 mg L^{-1} (high EPS). These lethal concentrations are significantly lower than those for *E. coli* grown in Luria–Bertani medium (6.35 mg L^{-1}),[24] which contains a relatively high chloride concentration (10 g L^{-1}) that promotes precipitation of AgCl and decreases the bioavailable Ag^+ concentration.[4]

Formation of AgNPs from Ag^+ Reduction. Figure 2A shows a TEM image of *E. coli* exposed to Ag^+ (0.165 mg L^{-1})

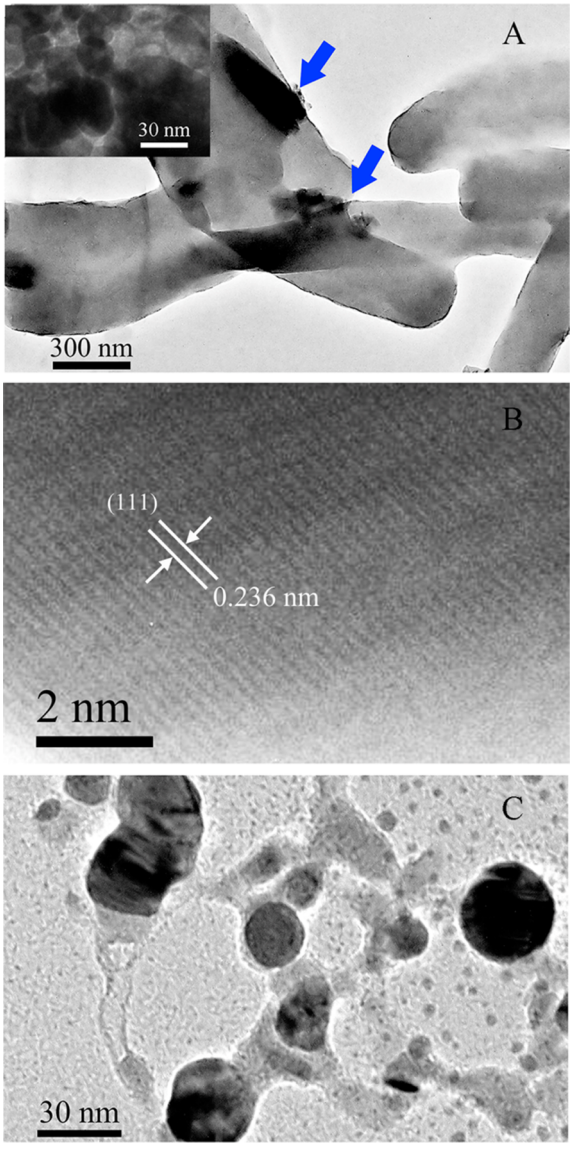

Figure 2. TEM images of AgNPs formed from Ag^+ (0.165 mg L^{-1}). (A) AgNPs formed in the presence of *E. coli* (1.0×10^7 cell mL^{-1}). Arrows point to the AgNPs (10–30 nm in diameter), amplified in the upper-left corner. (B) HRTEM lattice-fringe fingerprinting of these AgNPs. The interplanar spacing (0.236 nm) is consistent with the crystal face of element silver. (C) AgNPs formed *in vitro* with aqueous EPS (200 mg L^{-1}).

for 16 h, with clustered silver particles (10–30 nm in diameter) accumulating on the cell surface. SAED analysis (see Figure S2 of the Supporting Information) indicates that these nanoparticles had an identical pattern to that of metallic silver crystal; these nanoparticles show a pattern of polycrystalline rings, indexed to the cubic crystal structure of metallic silver.[25] Furthermore, HRTEM analysis reflects that the measured interplanar spacing (0.236 nm) of the lattice-fringe fingerprinting of the nanoparticles is consistent with the crystal face of elemental metallic silver (Figure 2B). AgNPs were also produced *in vitro* from Ag^+ in the presence of aqueous EPS (200 mg L^{-1}) (Figure 2C), which was similarly corroborated by SAED combined with HRTEM analyses. The formation of AgNPs from Ag^+ was also validated by XPS analysis (Figure 3).

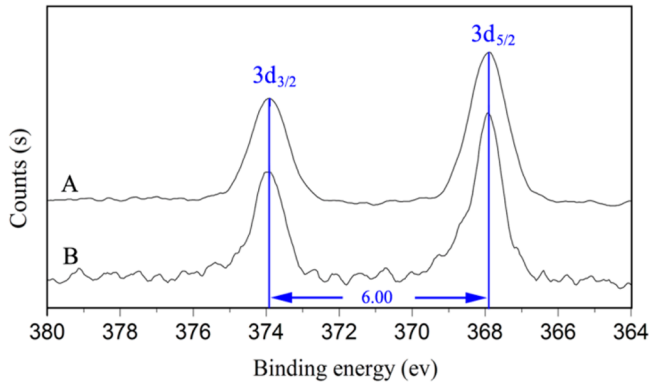

Figure 3. XPS analysis of AgNPs formed from Ag^+ (0.165 mg L^{-1}) in the presence of (A) *E. coli* cells (1.0×10^7 cell mL^{-1}) or (B) EPS (200 mg L^{-1}).

For both treatments (with live cells or *in vitro* with EPS), the binding energies in the Ag 3d region were observed at 373.9 and 367.9 eV, characteristic of the Ag 3d3/2 and Ag 3d5/2 signals of metallic silver.[26] The results of EDS analysis reaffirmed the formation of AgNPs from Ag^+ in the presence of *E. coli* cells (see Figure S3 of the Supporting Information).

Figure 4 presents the formation of AgNPs from Ag^+ at various aqueous EPS concentrations. As the EPS concentration increased from 40 to 200 mg L^{-1}, the color of the AgNPs formed in aqueous solutions changed from pale brown to reddish brown. Furthermore, the UV–vis absorbance of the AgNP samples showed a red shift in wavelength, with a maximum absorbance observed at 430 nm for 40 mg L^{-1} EPS, 440 nm for 100 mg L^{-1} EPS, and 470 nm for 200 mg L^{-1} EPS. Both the change to a darker color and the red shift in UV–vis absorbance suggest enhanced aggregation of AgNPs[22] with an increasing EPS concentration. No AgNPs were produced in the absence of EPS. Overall, these results provide unequivocal evidence that EPS can reduce Ag^+ to AgNPs and hinder intracellular penetration, hence antagonizing the bactericidal activity of Ag^+.

Fate of Ag^+ and AgNPs in *E. coli* Suspensions. After 16 h of incubation with different initial Ag^+ concentrations, Ag^+ was present in all compartments under consideration (i.e., the culture medium, EPS matrix, and inside cells), whereas AgNPs were found suspended in the medium and entrapped in EPS but not inside cells (Figure 5A). The recovery of total silver ranged from 94.6 to 105.3%. AgNPs in the culture medium and in the EPS matrix, as well as intracellular Ag^+ in the EPS matrix, exhibited similar bell-shaped mass distribution profiles, peaking when the added Ag^+ was 0.13 mg L^{-1}. In contrast, the concentration of Ag^+ in the culture medium was nearly constant or slightly increased up to 0.13 mg L^{-1} and then increased abruptly for higher initial Ag^+ concentrations. Accordingly, while AgNPs were the dominant silver species (55–60% of total silver) for treatments with less than 0.13 mg L^{-1} Ag^+, the predominant species was Ag^+ in culture medium

dx.doi.org/10.1021/es403796x | *Environ. Sci. Technol.* 2014, 48, 316–322

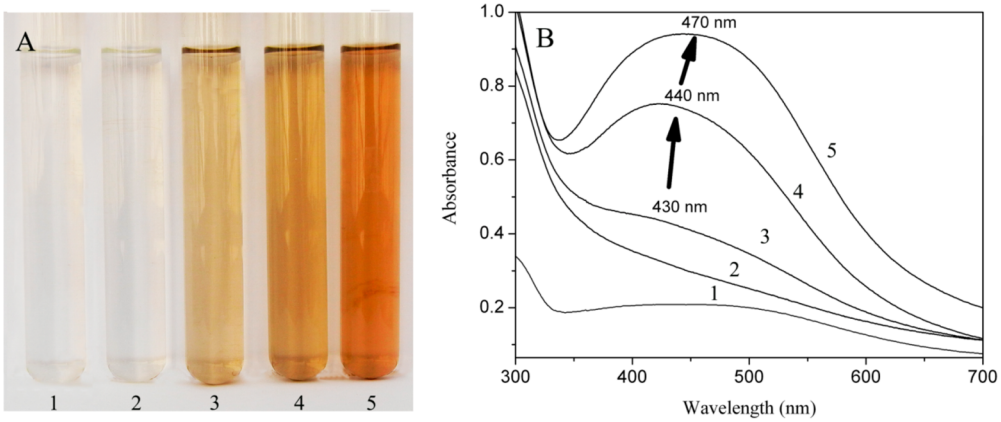

Figure 4. *In vitro* formation of AgNPs from Ag^+ (0.6 g L^{-1}) at various EPS concentrations. (A) Photograph of various suspensions. (B) UV−vis absorbance spectra. Sample 1 containing EPS (40 mg L^{-1}) but no Ag^+ and sample 2 containing 0.6 g L^{-1} Ag^+ but no EPS were shown for comparison. The arrows represent the red shift in wavelength as a result of the formation of AgNPs as the EPS concentration was increased from 40, 100, to 200 mg L^{-1} (samples 3, 4, and 5, respectively).

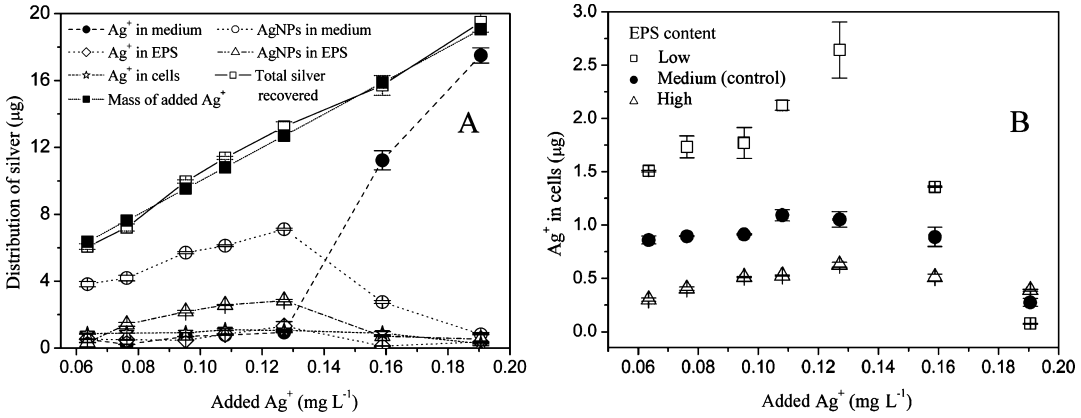

Figure 5. Fate of silver in *E. coli* suspensions (initially inoculated at 1.3×10^7 cell mL^{-1}) after 16 h of incubation. (A) Mass distribution of Ag^+ and AgNPs in culture medium, entrapped in EPS attached to cells, and inside cells. (B) Intracellular concentration of silver decreased with an increasing EPS content: low (i.e., EPS removed from suspension by sonication/centrifugation), medium (no manipulation of EPS content), and high (aqueous EPS added at 200 mg L^{-1}). Error bars represent standard deviations calculated from triplicate samples (those associated with the total silver recovered are calculated through error propagation).

(71−92% of total silver) at higher initial Ag^+ concentrations. Such high Ag^+ concentrations were toxic (Figure 1) and eliminated live cells as a potential sink. This inhibited EPS production, which, in turn, suppressed the formation of AgNPs from Ag^+, and Ag^+ in the cultural medium increased rapidly. Note that intracellular Ag^+ concentrations decreased with EPS content (Figure 5B), which further corroborates that EPS can serve as a permeability barrier that antagonizes the bactericidal activity of silver.

Ag^+ Reduction Mechanisms. Whereas Ag^+ reduction in various biological systems ranging from bacteria, fungus, to plants is possible,[33−36] little is known about which organic moieties and functional groups are involved and no previous study had considered Ag^+ reduction by EPS. Here, we show the involvement of reducing sugar components in EPS in Ag^+ reduction, by comparing the FTIR spectra of EPS before and after reaction with Ag^+ (Figure 6). For the pristine EPS (Figure 6A), the band at 1650 cm^{-1} is ascribed to the C═O stretching (amide I), while the band at 1550 cm^{-1} is ascribed to the N−H bending and C−N stretching (amide II) in peptides.[27,28] The band at 1457 cm^{-1} is ascribed to the deformation vibration of CH_2.[27] The bands at 1399 and 1385 cm^{-1} are related to the stretching of C−O and C═O, respectively, in carboxylate,[28,37]

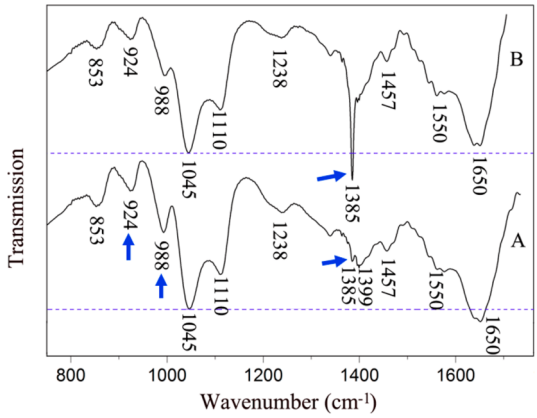

Figure 6. Comparison of FTIR spectra of EPS before and after reaction with Ag^+: (A) pristine EPS and (B) EPS reacted with Ag^+ (0.165 mg L^{-1}). Baselines (dashed) are set according to the stretching band of polysaccharide hydroxyl, which is inert to reaction with Ag^+.

while the band near 1238 cm^{-1} is related to the deformation vibration of C═O in carboxylic acid.[27] The bands near 1045 and 1110 cm^{-1} are assigned to the stretching of hydroxyl and

C−O−C, respectively, in polysaccharides.[28,29] The band at 988 cm^{-1} is related to the rhamnose components with two glycosidic linkage types of the furanoid compounds in saccharides.[30] The bands at 924 and 853 cm^{-1} are related to the rings of pyranose[31] and galactopyranose,[32] respectively, in polysaccharides. After reaction with Ag^+, the bands of rhamnose (988 cm^{-1}) and pyranose (924 cm^{-1}) structures become much weaker, whereas the band of carboxyl groups (1385 cm^{-1}) becomes much sharper and stronger (Figure 6B). This indicates that the aldehyde groups in these reducing sugars were oxidized to carboxyl groups by Ag^+. Consistently, a comparison of solution-phase ^{13}C NMR spectra of EPS before and after reaction with Ag^+ (results presented in Figure S4 of the Supporting Information) indicates that the hemiacetal groups of rhamnose (indicated by the peak at 100.8 ppm) were involved in Ag^+ reduction. Overall, these results imply that both the amount and content of reducing sugars produced can be important determinants of the bactericidal efficacy and potential environmental impacts of Ag^+.

■ ASSOCIATED CONTENT

Supporting Information

Results of the growth curve of *E. coli* (Figure S1), characterization of AgNPs by SAED (Figure S2) and EDS (Figure S3), and EPS by ^{13}C NMR (Figure S4). This material is available free of charge via the Internet at http://pubs.acs.org.

■ AUTHOR INFORMATION

Corresponding Author

*Telephone/Fax: +86-025-8968-0372. E-mail: zhud@nju.edu.cn.

Notes

The authors declare no competing financial interest.

■ ACKNOWLEDGMENTS

This work was supported by the National Science Foundation of China (Grants 21237002 and 21225729).

■ REFERENCES

(1) Chao, J. B.; Liu, J. F.; Yu, S. J.; Feng, Y. D.; Tan, Z. Q.; Liu, R.; Yin, Y. G. Speciation analysis of silver nanoparticles and silver ions in antibacterial products and environmental waters via cloud point extraction-based separation. *Anal. Chem.* **2011**, *83* (17), 6875−6882.

(2) Xiu, Z. M.; Zhang, Q. B.; Puppala, H. L.; Colvin, V. L.; Alvarez, P. J. J. Negligible particle-specific antibacterial activity of silver nanoparticles. *Nano Lett.* **2012**, *12* (8), 4271−4275.

(3) Ghandour, W.; Hubbard, J. A.; Deistung, J.; Hughes, M. N.; Poole, R. K. The uptake of silver ions by *Escherichia coli* K12: Toxic effects and interaction with copper ions. *Appl. Microbiol. Biotechnol.* **1988**, *28* (6), 559−565.

(4) Xiu, Z. M.; Ma, J.; Alvarez, P. J. J. Differential effect of common ligands and molecular oxygen on antimicrobial activity of silver nanoparticles versus silver ions. *Environ. Sci. Technol.* **2011**, *45* (20), 9003−9008.

(5) Teitzel, G. M.; Parsek, M. R. Heavy metal resistance of biofilm and planktonic *Pseudomonas aeruginosa*. *Appl. Environ. Microb.* **2003**, *69* (4), 2313−2320.

(6) Ivleva, N. P.; Wagner, M.; Horn, H.; Niessner, R.; Haisch, C. In situ surface-enhanced raman scattering analysis of biofilm. *Anal. Chem.* **2008**, *80* (22), 8538−8544.

(7) Vu, B.; Chen, M.; Crawford, R. J.; Ivanova, E. P. Bacterial extracellular polysaccharides involved in biofilm formation. *Molecules* **2009**, *14* (7), 2535−2554.

(8) Bhaskar, P. V.; Bhosle, N. B. Microbial extracellular polymeric substances in marine biogeochemical processes. *Curr. Sci. India* **2005**, *88* (1), 45−53.

(9) Wingender, J.; Neu, T. R.; Flemming, H. C. *Microbial Extracellular Polymeric Substances: Characterization, Structure, and Function*; Springer-Verlag: Berlin, Germany, 1999.

(10) Cao, B.; Ahmed, B.; Kennedy, D. W.; Wang, Z.; Shi, L.; Marshall, M. J.; Fredrickson, J. K.; Isern, N. G.; Majors, P. D.; Beyenal, H. Contribution of extracellular polymeric substances from *Shewanella* sp. HRCR-1 biofilms to U(VI) immobilization. *Environ. Sci. Technol.* **2011**, *45* (13), 5483−5490.

(11) Harish, R.; Samuel, J.; Mishra, R.; Chandrasekaran, N.; Mukherjee, A. Bio-reduction of Cr(VI) by exopolysaccharides (EPS) from indigenous bacterial species of Sukinda chromite mine, India. *Biodegradation* **2012**, *23* (4), 487−496.

(12) Comte, S.; Gulbaud, G.; Baudu, M. Biosorption properties of extracellular polymeric substances (EPS) resulting from activated sludge according to their type: Soluble or bound. *Process Biochem.* **2006**, *41* (4), 815−823.

(13) Lowry, O. H.; Rosebrough, N. J.; Farr, A. L.; Randall, R. J. Protein measurement with the folin phenol reagent. *J. Biol. Chem.* **1951**, *193* (1), 265−275.

(14) Frolund, B.; Griebe, T.; Nielsen, P. H. Enzymatic activity in the activated-sludge floc matrix. *Appl. Microbiol. Biotechnol.* **1995**, *43* (4), 755−761.

(15) Dubois, M.; Gilles, K. A.; Hamilton, J. K.; Rebers, P. A.; Smith, F. Colorimetric method for determination of sugars and related substances. *Anal. Chem.* **1956**, *28* (3), 350−356.

(16) Burton, K. A study of the conditions and mechanism of the diphenylamine reaction for the colorimetric estimation of deoxyribonucleic acid. *Biochem. J.* **1956**, *62* (2), 315−323.

(17) Liu, H.; Fang, H. H. P. Extraction of extracellular polymeric substances (EPS) of sludges. *J. Biotechnol.* **2002**, *95* (3), 249−256.

(18) Duffy, G.; O'Brien, S. B.; Carney, E.; Sheridan, J. J.; McDowell, D. A.; Blair, I. S. Characterisation of *E. coli* O157 isolates from bovine hide and beef trimming in Irish abattoirs by pulsed field gel electrophoresis. *J. Microbiol. Methods* **2005**, *60* (3), 375−382.

(19) Begot, C.; Desnier, I.; Daudin, J. D.; Labadie, J. C.; Lebert, A. Recommendations for calculating growth parameters by optical density measurements. *J. Microbiol. Methods* **1996**, *25* (3), 225−232.

(20) Liu, J. F.; Chao, J. B.; Liu, R.; Tan, Z. Q.; Yin, Y. G.; Wu, Y.; Jiang, G. B. Cloud point extraction as an advantageous preconcentration approach for analysis of trace silver nanoparticles in environmental waters. *Anal. Chem.* **2009**, *81* (15), 6496−6502.

(21) Yu, S. J.; Chao, J. B.; Sun, J.; Yin, Y. G.; Liu, J. F.; Jiang, G. B. Quantification of the uptake of silver nanoparticles and ions to HepG2 cells. *Environ. Sci. Technol.* **2013**, *47* (7), 3268−3274.

(22) Yin, Y.; Liu, J.; Jiang, G. Sunlight-induced reduction of ionic Ag and Au to metallic nanoparticles by dissolved organic matter. *ACS Nano* **2012**, *6* (9), 7910−7919.

(23) Cheng, Y. J.; Yan, F. B.; Huang, F.; Chu, W. S.; Pan, D. M.; Chen, Z.; Zheng, J. S.; Yu, M. J.; Lin, Z.; Wu, Z. Y. Bioremediation of Cr(VI) and immobilization as Cr(III) by *Ochrobactrum anthropi*. *Environ. Sci. Technol.* **2010**, *44* (16), 6357−6363.

(24) Feng, Q. L.; Wu, J.; Chen, G. Q.; Cui, F. Z.; Kim, T. N.; Kim, J. O. A mechanistic study of the antibacterial effect of silver ions on *Escherichia coli* and *Staphylococcus aureus*. *J. Biomed. Mater. Res.* **2000**, *52* (4), 662−668.

(25) He, Y.; Zhang, Z.; Hoffmann, C.; Zhao, Y. Embedding Ag nanoparticles into MgF_2 nanorod arrays. *Adv. Funct. Mater.* **2008**, *18* (11), 1676−1684.

(26) Wagner, C. D; Riggs, W. M.; Davis, L. E.; AMoulder, J. F. *Handbook of X-ray Photoelectron Spectroscopy: A Reference Book of Standard Data for Use in X-ray Photoelectron Spectroscopy*; Perkin-Elmer: Minneapolis, MN, 1979.

(27) Guibaud, G.; Tixier, N.; Bouju, A.; Baudu, M. Relation between extracellular polymers' composition and its ability to complex Cd, Cu and Pb. *Chemosphere* **2003**, *52* (10), 1701−1710.

(28) Guibaud, G.; Comte, S.; Bordas, F.; Dupuy, S.; Baudu, M. Comparison of the complexation potential of extracellular polymeric substances (EPS), extracted from activated sludges and produced by pure bacteria strains, for cadmium, lead and nickel. *Chemosphere* **2005**, *59* (5), 629−638.
(29) Comte, S.; Guibaud, G.; Baudu, M. Relations between extraction protocols for activated sludge extracellular polymeric substances (EPS) and EPS complexation properties: Part I. Comparison of the efficiency of eight EPS extraction methods. *Enzyme Microb. Technol.* **2006**, *38* (1−2), 237−245.
(30) Kacurakova, M.; Capek, P.; Sasinkova, V.; Wellner, N.; Ebringerova, A. FT-IR study of plant cell wall model compounds: Pectic polysaccharides and hemicelluloses. *Carbohydr. Polym.* **2000**, *43* (2), 195−203.
(31) Guo, J. Y.; Zhang, X. M. Metal−ion interactions with sugars. The crystal structure and FTIR study of an $SrCl_2$−fructose complex. *Carbohydr. Res.* **2004**, *339* (8), 1421−1426.
(32) Koshy, K. M.; Boggs, J. M. The effect of anomerism and hydration on the C−O−S vibrational frequency of D-galactose-3-sulfate determined by FTIR spectroscopy. *Carbohydr. Res.* **1997**, *297* (2), 93−99.
(33) Shankar, S. S.; Ahmad, A.; Sastry, M. Geranium leaf assisted biosynthesis of silver nanoparticles. *Biotechnol. Prog.* **2003**, *19* (6), 1627−1631.
(34) Shahverdi, A. R.; Minaeian, S.; Shahverdi, H. R.; Jamalifar, H.; Nohi, A. A. Rapid synthesis of silver nanoparticles using culture supernatants of *Enterobacteria*: A novel biological approach. *Process Biochem.* **2007**, *42* (5), 919−923.
(35) Parikh, R. Y.; Singh, S.; Prasad, B. L. V.; Patole, M. S.; Sastry, M.; Shouche, Y. S. Extracellular synthesis of crystalline silver nanoparticles and molecular evidence of silver resistance from *Morganella* sp.: Towards understanding biochemical synthesis mechanism. *ChemBioChem* **2008**, *9* (9), 1415−1422.
(36) Mukherjee, P.; Ahmad, A.; Mandal, D.; Senapati, S.; Sainkar, S. R.; Khan, M. I.; Parishcha, R.; Ajaykumar, P. V.; Alam, M.; Kumar, R.; Sastry, M. Fungus-mediated synthesis of silver nanoparticles and their immobilization in the mycelial matrix: A novel biological approach to nanoparticle synthesis. *Nano Lett.* **2001**, *1* (10), 515−519.
(37) Terkhi, M. C.; Taleb, F.; Gossart, P.; Semmoud, A.; Addou, A. Fourier transform infrared study of mercury interaction with carboxyl groups in humic acids. . *J. Photochem. Photobiol., A* **2008**, *198*, 205−214.